ACI JOURNAL TECHNICAL PAPER

Title no. 76-46

Concrete Columns Under Biaxially Eccentric Thrust

by Richard W. Furlong

Data from biaxially eccentric load tests of 9 specimens with a 5 x 9 in. (130 x 230 mm) rectangular cross section plus 14 specimens with a 5 x 11 in. (130 x 280 mm) rounded end cross section are reported as a supplement to data already available from others for tests on square columns. Cross section strength analyses derived with the traditional rectangular stress block to represent concrete were found to underestimate observed capacities. Improved correlation between analysis and observation required the use of a nonlinear stress-strain function for concrete that remained unspalled until maximum surface strains reached at least 0.4 percent. Slenderness effects from biaxial bending were governed largely by weak axis flexibility, and significant differences were observed between the skew angle of the neutral axis and the skew angle of the eccentric load. However, no twisting about the longitudinal axis was detected. Moment magnification factors if used for design in accordance with ACI Building Code recommendations determined separately for each principal axis of bending would have produced safe results. The elliptical relationship of ratios between bending moment and bending capacities about each principle axis produced strength estimates that averaged 10 percent greater than measured strength. The Bresler reciprocal thrust formulation of capacity produced results always safe, but results that averaged 26 percent above measured capacity.

Keywords: bending; **biaxial loads; columns (supports);** compression tests; compressive strength; **eccentric loads;** failure; live loads; loads (forces) slenderness ratio; stiffness; stress block; stress-strain relationships; **structural analysis;** structural design.

Received Jan. 31, 1979, and reviewed under Institute publication policies. Pertinent discussion will be published in the August 1980 ACI JOURNAL if received by Apr. 1, 1980.

Richard W. Furlong, FACI, is Professor of Civil Engineering at the University of Texas at Austin. He has served ACI as a Director and as a member of committees on Columns, Inelastic Response of Structures, Strength Handbook, and Nomenclature.

ABSTRACT

Data from biaxially eccentric load tests of 9 specimens with a 5 x 9 inch (130 x 230 mm) rectangular cross section plus 14 specimens with a 5 x 11 inch (130 x 280 mm) rounded end cross section are reported as a supplement to data already available from others for tests on square columns. Cross section strength analyses derived with the traditional rectangular stress block to represent concrete were found to underestimate observed capacities. Improved correlation between analysis and observation required the use of a non-linear stress-strain function for concrete that remained unspalled until maximum surface strains reached at least 0.4 per cent. Slenderness effects from biaxial bending were governed largely by weak axis flexibility, and significant differences were observed between the skew angle of the neutral axis and the skew angle of the eccentric load. However, no twisting about the longitudinal axis was detected. Moment magnification factors if used for design in accordance with ACI Building Code recommendations determined separately for each principal axis of bending would have produced safe results. The elliptical relationship of ratios between bending moment and bending capacities about each principal axis produced strength estimates that averaged 10% greater than measured strength. The Bresler reciprocal thrust formulation of capacity produced results always safe, but results that averaged 26% below measured capacity.

INTRODUCTION

Design criteria for eccentrically loaded concrete columns during the past half century have evolved from allowable stress limits for presumably elastic members toward strength limits that recognize inelastic material response before maximum strength is achieved. Early recognition that compression stress limits at the extreme fibers of concrete cross sections produced unacceptably low estimates of allowable load preceded the adoption of a strength formulation of an allowable stress for the design of non-slender axially loaded columns (1). Analysis for flexure in addition to thrust continued to require an elastic analysis of the heterogeneous cross sections. If design loading required resistance to biaxially eccentric thrust, a complex analysis of elastic response was necessary (2), and an allowable stress limit governed the design. The procedure certainly was safe, and the difficult analysis (sans electronic computers) was avoided if a rationale for alternate load cases could be cited as a basis for designing the column. Graphs or

tables were available as a computation aid for eccentric loads in the plane of a principal axis of cross sections (3).

The application of strength criteria as a basis for designing concrete columns would be more complex analytically than the elastic strain and allowable stress criteria had been were it not for the rectangular stress block representation of concrete at ultimate. The accepted use of a constant ultimate stress equal to 85 percent of the cylinder strength f'_c on a compression zone extending from the extreme fiber 85 per cent of the depth to a neutral axis (4) made strength analysis of beam columns no more difficult than the allowable stress analysis had been. Under biaxially eccentric loading conditions the use of the rectangular stress block for concrete at ultimate made the strength analysis less complex than the elastic stress analysis procedure.

However, when failure of a cross section analytically is defined to occur when any strain reaches 0.3 per cent and when the rectangular stress block is used to represent concrete strength at ultimate, the accuracy of the capacity calculation decreases as the strain gradient decreases. (The strain gradient is the quotient obtained when extreme fiber strain is divided by the distance between the extreme fiber and the neutral axis.) The use of the rectangular stress block undervalues flexural strength if cross sections contain little or no tensile strain regions at failure (5). The characteristic thrust-moment interaction diagram should "bulge out" somewhat with larger values of moment when thrust is between 25 to 75 per cent of the squash load P_o. Since strength analytically is undervalued for cross sections with an entire edge at the same failure strain, possibly it could be undervalued even more if only a corner were subjected to the maximum strain.

Computer programs have been developed for analyzing the behavior of columns composed of discrete elements of dissimilar materials with stress-strain functions that can be specified or programmed (6, 7). Results from the analytical treatment reported by Farah and Huggins were shown by Drysdale (8) to agree well with results observed from tests on square columns. The analytic treatments included displacement estimates as stresses or loads increase. Wu reported (9) that the Farah and Huggins program gave good predictions of secondary beam column effects caused by the lateral displacements of biaxially loaded long columns. A specific discrete element analysis of column cross sections is not a practical tool for design. For design practice, graphs or computer subroutines that produce analytic estimates for "standard" materials and cross section shapes are necessary.

Almost all columns that support bridges must be designed to resist load combinations that create significant amounts of biaxial bending, but biaxial bending is rarely a critical concern for the design of columns in buildings. Even though every column in every building resists biaxially eccentric thrust most of the time, the limit loading conditions that serve as a basis for structural design are derived from an analysis of frames in the planes in which the principal axes of columns are constructed. Column design moments are largest when live load exists in the bay adjacent to a column only in the direction of maximum moment as suggested in Fig. 1. As live load is shifted from principal axes to a skew axis of bending as in Fig. 1(b) to produce maximum skewed bending, the reduction in the effective span across skewed lines leaves a resultant skewed moment which is less than the moment that could be produced about either principle axis by the same unit loading. Only at the exterior corner of a building does maximum skew bending occur under the same loading that creates maximum moment about each principal axis. The type of framing sometimes eliminates significant skew bending possibilities even at corner columns of buildings.

The ACI Building Code (10) and the AASHTO criteria (11) explicitly recognize the use of the rectangular stress block and a fiber failure strain limit of 0.3 per cent to represent concrete in the analysis of cross section strength. More sophisticated representations of the stress-strain behavior of concrete are permitted, but only the rectangular stress block is used for the derivation of design aids that are readily available (12, 13, 14). The design aids are applicable for the strength design of cross sections, presumably after moment magnifiers from slenderness effects have been investigated for secondary moments acting separately about each principal axis. Additional secondary effects, such as twisting instability unique to conditions of biaxially eccentric thrust, are not ordinarily considered for design.

Rectangular cross section capacity is derived from analytical representations of an interaction surface for which thrust capacity is the vertical abscissa and bending capacities about each principal axis are horizontal ordinates. Contours at constant thrust have been described (14, 15) as an elliptic function of the ratios between moment components and moment capacities about each principal axis in the form

$$\left(\frac{m_x}{M_x}\right)^{\eta} + \left(\frac{m_y}{M_y}\right)^{\eta} = 1. \qquad (1)$$

The magnitude of the exponent η has an upper limit value of 2 when thrust equals the squash load P_o, and the magnitude of η decreases to reflect variables such as the reinforcement ratio, the ratio between the short side and the long side of the rectangle, and the ratio between concrete strength and steel yield

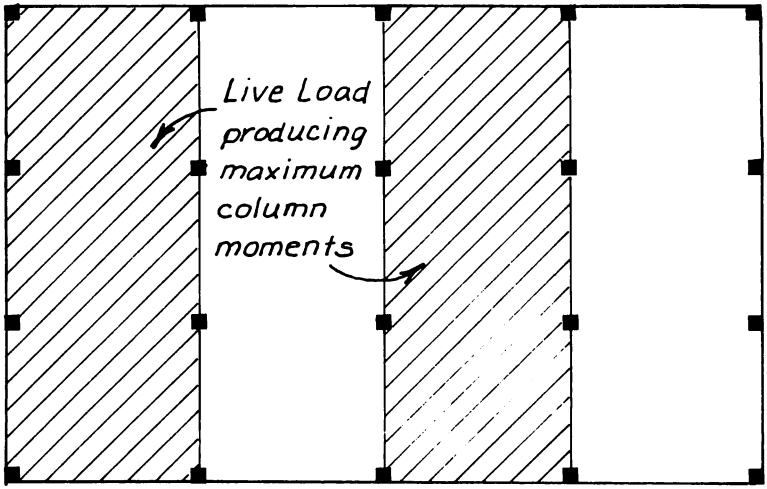

(a) Maximum Moments About a Major Axis

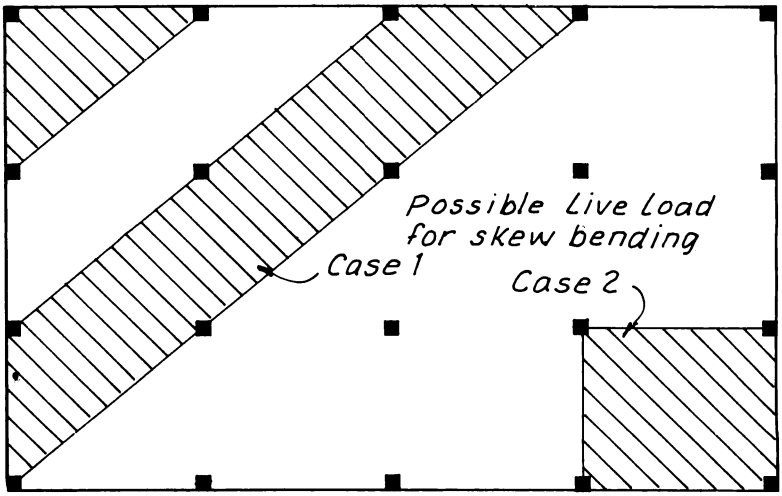

(b) Maximum Moments About a Skewed Axis

Fig. 1--Floor loading for maximum column moments

strength f'_c/f_y.

The form of Eq. (1) is convenient, but the apparent precision of accommodating numerous parameters is not appropriate for the real accuracy of the equation. The design aids (14, 15) for determining the exponent η were derived from computer programs that used the rectangular stress block and a limit strain to define concrete at ultimate load. That analytic model for concrete behavior at ultimate may differ from the actual behavior of concrete enough to produce for Eq. (1) errors in strength estimates that are greater than errors that result from changes of parameters such as f'_c and f_y, reinforcement ratios, or ratios between the length of sides of rectangles. Present design procedures may be more cumbersome than their consequent accuracy can justify.

The major goal of this study was to recommend for biaxially loaded concrete columns a design procedure for which the accuracy of calculations would be comparable with the precision of results. It was beyond the scope of this study to refine existing strength analysis procedures for columns eccentrically loaded in a principal plane. The majority of physical tests of eccentrically loaded columns have involved square shapes, and no new tests of square cross sections were included in this study. In order to provide data relevant for the proportions of columns used for highway bridges, a rectangular section and a rounded end cross section were tested.

LABORATORY TESTS

A testing program for non-square columns under biaxially eccentric thrust was carried out on specimens slender enough to deform laterally during the application of load (16). In addition to the desire to test bridge column shapes it was felt that secondary deformations that are unique for biaxially loaded beam columns might be revealed more readily by observations of columns with cross-sections that have bending flexibilities quite different about each principal axis than by observations of square columns.

Specimens with a 5 x 9-in. (130 x 230 mm) rectangular cross section and specimens with a 5 x 11-in. (130 x 280 mm) rounded end cross section are described in Fig. 2. The latter cross section was designed to model a configuration familiar for single column bridge piers. The low reinforcement ratio employed for all specimens also is characteristic for concrete bridge structures. The 72-in. (1830 mm) long specimens were subjected to an axial force that was maintained constant while bending moments were applied in increasing amounts until failure occurred. Measurements of longitudinal strain and lateral displacement along the length of each loaded specimen were used for evidence of secondary beam-column response.

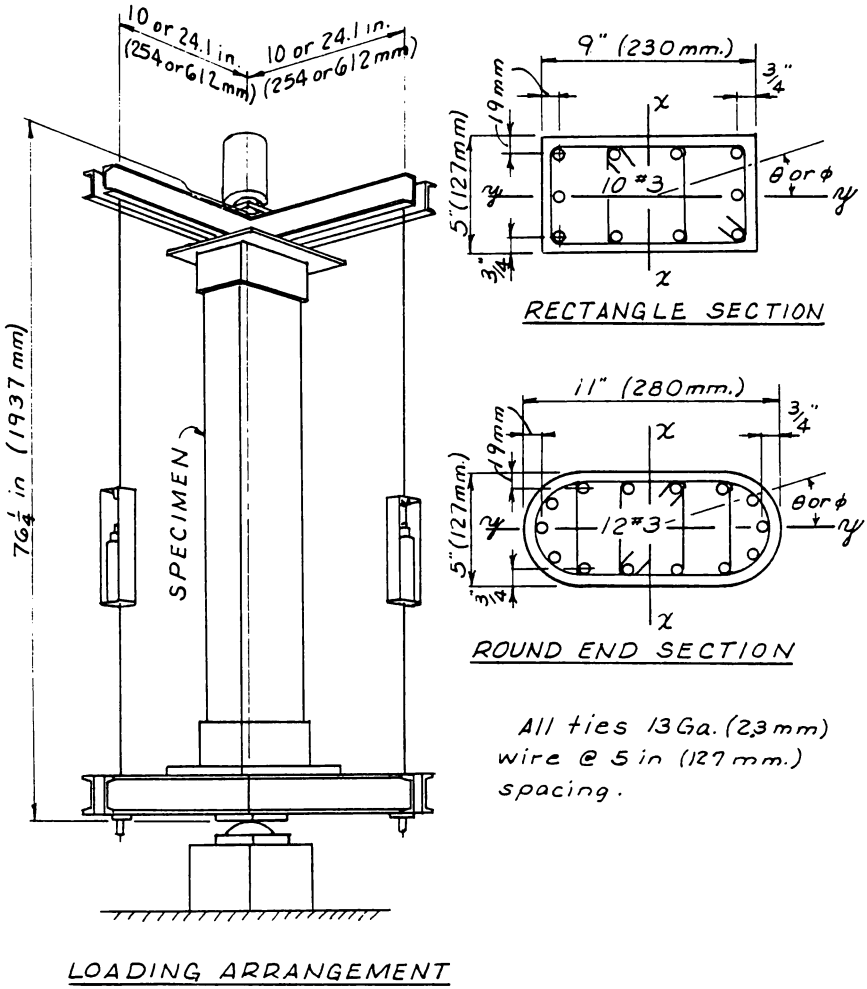

Fig. 2--Test specimens

Three different levels of thrust were applied while moments were increased at 3 different nominal angles of skewed bending. At each of the 3 levels of thrust bending moments were applied in the plane of each principal axis of rounded end specimens only. It was assumed that an adequate amount of data already exists for uniaxially eccentric loads on rectangular cross sections. The three levels of thrust were set at approximately one sixth, one third and one half of the nominal squash load P_o for each specimen. Biaxially eccentric thrusts at higher fractions of P_o would involve very small resultant eccentricities for which analysis has indicated that an elliptical function describes adequately the interaction surface. Forces were applied to specimens through a loading head that consisted of a rigid steel box to which were welded the beams on which flexural forces could be applied. A hemisphere shaped bearing was applied to the center of the rigid box, and most of the applied axial force acted through the hemispherical bearing. As flexural loads were increased the force on the hemispherical bearings was reduced in order that the total axial force would remain constant.

Longitudinal strains were monitored with displacement gages opposite the 4 faces of each specimen. The longitudinal strain meters were located 6 inches apart at 5 stations symmetric about midheight of each column. Lateral displacements in the directions of the principal axes also were monitored at 7 stations along the length of the specimens. Rotations were measured at mid-height and at each end of the specimen. As failure appeared to be imminent, all gage readings were recorded, and subsequent loading increments were made smaller. Nevertheless, the majority of failures were sudden, and some of the measuring equipment was damaged as the column failures took place.

TEST RESULTS

The nominal specimen dimensions, concrete quality f'_c, computed squash load P_o, failure thrust, failure moments, failure skew angles, and maximum measured longitudinal strain for each of the 14 specimens are listed in Table A. At each end of the specimens the nominal moment loading devices created the major portion of end moments that are tabulated. Small eccentricities of the loading head spherical balls at the ends of specimens were computed analytically from displacement curve data accumulated during each test. The tabulated values of end moment include the effects of specimen and loading head alignment corrections and represent the average of the end moments at each end of the specimen. Midheight moments were larger than end moments as the specimens deformed under applied loading.

Longitudinal strain meters had a 6-inch gage length, and the meters produced readings of longitudinal deformations opposite each face of the columns. Among the 4 readings of strain at any cross section, only 3 could be used to define a plane. Planes defined by 3 readings were checked against the

TABLE A1 - Specimens and Failure Forces - Customary Units

Specimen	Size	f'_c	Calc. P_o	Failure P_u	End of Specimen			Midheight				Max. Measured Strain
					M_x	M_y	Skew ∠ θ	M_{ux}	M_{uy}	Skew ∠ θ	Neutral Axis ∠ ϕ	
	(in. × in.)	ksi	k	k	in-k	in-k	degree	in-k	in-k	degree	degree	%
R1	5 × 9 Rectangle	4.89	220.	119.	47.5	123.7	21.0	60.6	184.0	18.2	8.5	0.324
R2		4.87	219.	120.	107.5	89.5	50.2	124.0	154.1	38.8	16.2	0.438
R3		5.18	230.	129.	195.0	64.4	71.7	229.	127.4	60.9	28.1	0.499
R4		5.01	224.	87.1	34.0	98.1	19.1	40.3	160.8	14.1	4.6	0.314
R5		5.21	232.	94.3	114.2	96.7	49.7	128.2	150.4	40.4	16.1	0.366
R6		4.70	212.	85.8	190.7	62.1	72.0	218.	102.0	64.9	31.9	0.514
R7		4.43	202.	53.9	429.	100.2	25.5	52.2	145.9	19.7	5.6	0.313
R8		4.35	199.	40.4	78.1	86.5	42.1	86.6	121.3	35.5	12.7	0.467
R9		4.45	203.	40.4	175.7	66.0	69.4	190.4	86.4	65.6	32.5	0.487
B1	5 × 11 Rounded Ends	4.46	234.	136.	0	93.8	0	0	154.1	0	–	0.526
B2		4.42	232.	138.	43.5	106.0	22.3	57.1	188.0	16.9	5.8	0.435
B3		4.40	231.	140.	142.2	85.9	58.9	165.1	161.6	45.6	12.7	0.357
B4		5.40	273	153.	233.	91.3	68.6	268.	147.7	61.1	23.2	0.392
B5		4.83	248.	156.	376	0	90.	424.	0	90.	–	0.347
B6		5.47	276.	109.	0	109.1	0	0	194.2	0.	–	0.309
B7		4.83	237.	96.2	59.1	109.7	28.3	67.8	179.1	20.7	4.8	0.357
B8		4.40	231.	92.2	147.0	98.3	56.2	171.3	142.1	49.3	14.1	0.306
B9		5.09	260	99.2	212.	99.2	64.9	243.	155.6	57.4	20.0	0.390
B10		5.51	278.	119.	402.	0	90.	455.	0	90.	–	0.526
B11		4.78	247.	60.7	0	120.8	0	0	165.5	0	–	0.401
B12		4.76	246.	57.1	59.2	121.6	26.0	64.4	168.0	21.0	3.7	0.353
B13		4.83	249.	53.2	232.	95.1	67.7	252.	128.8	62.9	21.1	0.420
B14		4.39	237.	58.4	338.	0	90.	372.	0	90.	–	0.381

TABLE A2 - Specimens and Failure Forces - SI Units

Specimen	Size	f'_c	Calc. P_o	Failure P_u	End of Specimen			Midheight				Max. Measured Strain
					M_x	M_y	Skew $\chi\theta$	M_{ux}	M_{uy}	Skew $\chi\theta$	Neutral Axis $\chi\phi$	
	(mm×mm)	MPa	kN	kN	kN-m	kN-m	degree	kN-m	kN-m	degree	degree	%
R1	127×229 Rectangle	33.7	990.	536.	5.42	14.10	21.0	6.91	21.0	18.2	8.5	0.324
R2		33.6	986.	540.	12.26	10.20	50.2	14.14	17.56	38.8	16.2	0.438
R3		35.7	1035.	580.	22.2	7.34	71.7	26.1	14.52	60.9	28.1	0.499
R4		34.5	1008.	392.	3.88	11.18	19.1	4.59	18.33	14.1	4.6	0.314
R5		35.9	1044.	424.	13.02	11.02	49.7	14.61	17.15	40.4	16.1	0.366
R6		32.4	954.	386.	21.7	7.08	72.0	24.8	11.63	64.9	31.9	0.514
R7		30.5	909.	243.	48.9	11.42	25.5	5.95	16.63	19.7	5.6	0.313
R8		30.0	896.	182.	8.90	9.86	42.1	9.87	13.83	35.5	12.7	0.467
R9		30.7	914.	182.	20.0	7.52	69.4	21.7	9.85	65.6	32.5	0.487
B1	127×279 Rounded Ends	30.7	1053.	612.	0	10.70	0	0	17.57	0	–	0.526
B2		30.5	1044.	621.	4.96	12.08	22.3	6.51	21.4	16.9	5.8	0.435
B3		30.3	1040.	630.	16.21	9.79	58.9	18.82	18.42	45.6	12.7	0.357
B4		37.2	1229.	688.	25.6	10.41	68.6	30.6	16.83	61.1	23.2	0.392
B5		33.3	1116.	702.	42.9	0	90.	48.3	0	90.	–	0.347
B6		37.7	1242.	490.	0	12.44	0	0	21.2	0.	–	0.309
B7		33.3	1066.	433.	6.74	12.51	28.3	7.73	20.4	20.7	4.8	0.357
B8		30.3	1040.	415.	16.76	11.21	56.2	19.53	16.20	49.3	14.1	0.306
B9		35.1	1170.	446.	24.2	11.31	64.9	27.7	17.74	57.4	20.0	0.390
B10		38.0	1251.	536.	45.8	0	90.	51.9	0	90.	–	0.526
B11		32.9	1112.	273.	0	13.77	0	0	18.87	0	–	0.401
B12		32.8	1107.	257.	6.75	13.86	26.0	7.34	19.15	21.0	3.7	0.353
B13		33.3	1120.	239.	26.4	10.84	67.7	28.7	14.68	62.9	21.1	0.420
B14	"	30.2	1066.	263.	38.5	0	90.	42.4	0	90.	–	0.381

4th reading and found to produce an average discrepancy less than 2 per cent of the 4th measurement just before specimens failed. The analytic assumption that plane sections remain plane after skew bending appeared to be valid. Recorded values of maximum strain listed in Table A were computed from the last recorded set of readings for the 6-inch gage station nearest the region at which spalling of concrete preceded failure.

The tabulated values of skew angle were calculated as the inverse tangent of the ratio between strong axis moment M_x and weak axis moment M_y. The neutral axis angles shown represent angles between the minor axis (the Y axis in Fig. 2) and the neutral axis as computed from longitudinal strains through the midheight region of the test specimens prior to failure. Values of skew angle near midheight were always smaller than values of skew angle at the ends because secondary moments due to lateral deflections obviously increased more for bending about the weak axis than about the strong axis.

The difference between skew angle θ and neutral axis angle ϕ appeared to increase as the angle itself increased. When bending occurs only about the minor axis, the neutral axis angle should be zero. Small changes of a few degrees would lead to only minor amounts of major axis bending. When bending occurs only about the major axis, the neutral axis angle should be 90 degrees. Even large "errors" of 20 to 30 degrees would produce only small amounts of minor axis bending. The graph of Fig. 3 indicates that the differences $\theta - \phi$ increased almost in direct proportion to the skew angle. Even though differences between skew angle and neutral axis angle suggest a tendency to twist, the largest amount of twist observed between midheight and ends of a specimen was 0.43 degrees for specimen R2. The consequent torsional stress index of 170 psi was comfortably lower than the torsional cracking strength of the cross section. Secondary torsional stresses due to skew bending would appear to be negligible unless slenderness ratios are significantly larger than those used for the test specimens.

ANALYSIS OF CROSS SECTION STRENGTH

Just before failure occurred the plane of strain that was established from the average of the 5 sets of strain meters throughout the 30-inch midheight zone of test specimens was used analytically as the failure plane for the specimen involved. The integration of stresses produced across a discretized analytical representation of the cross section yielded values of thrust and values of moment about each principal axis. A study was made to compare analytical forces with measured forces as several functions (17, 18, 19) shown in Fig. 4 were employed to define the stress-strain behavior of concrete. Results of the study are shown in Table B.

All calculated values of thrust and all but one value of moment were underestimated by analytical representations of

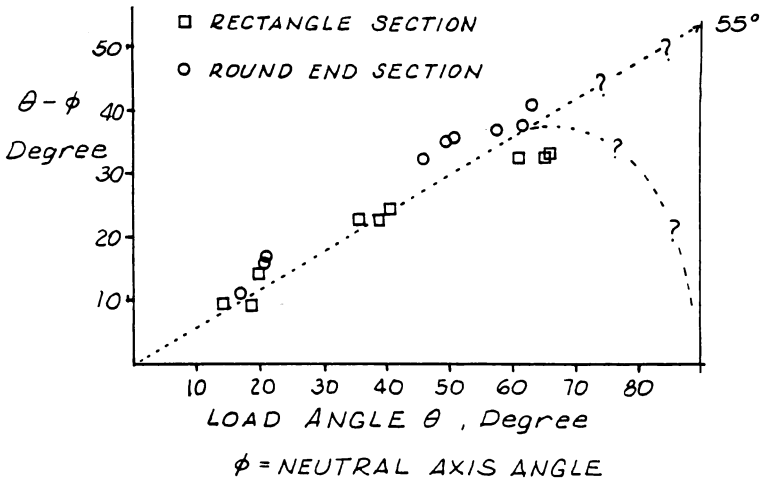

Fig. 3--Load angle and neutral axis angle

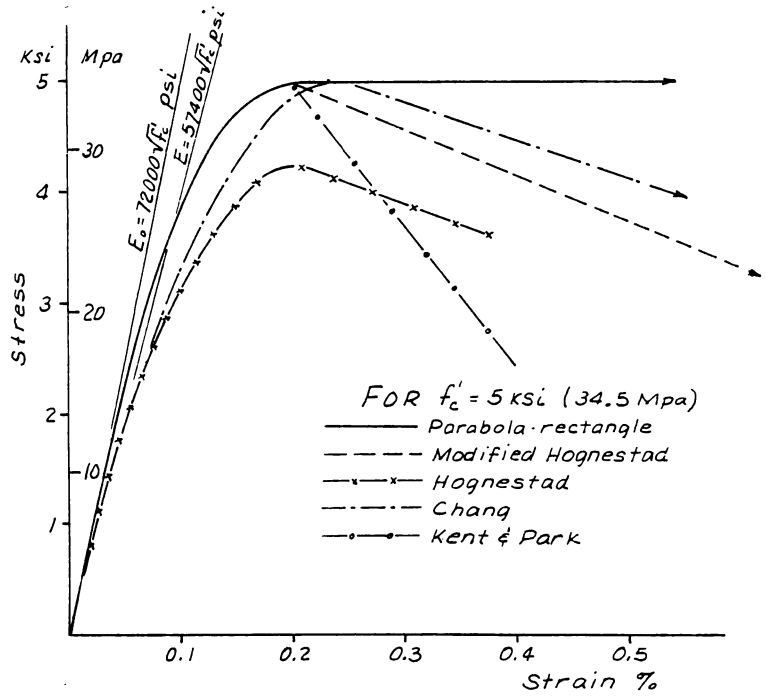

Fig. 4--Concrete stress-strain functions

TABLE B Observed Loads and Loads Computed from Strains

Specimen	Observed Forces			Ratio = Computed Value / Observed Value											
				Parabola-Rect.			Mod. Hognestad			Chang			Kent & Park		
	P_u K.	M_x K-ft	M_y K-ft	P_u	M_x	M_y	P_u	M_x	M_y	P_u	M_x	M_y	P_u	M_x	M_y
R1	119	60.6	184	.907	.981	.842	.908	.946	.834	.841	.971	.809	.884	.877	.809
R2	120	124	154.1	.876	.924	.938	.872	.890	.922	.811	.904	.898	.838	.821	.878
R3	129	229	127.4	.769	.894	.921	.755	.869	.895	.700	.854	.876	.725	.814	.840
R4	87.1	40.3	160.8	.799	.860	.970	.799	.838	.968	.724	.856	.917	.786	.796	.953
R5	94.3	128.2	150.4	1.002	.940	.986	.991	.918	.972	.905	.914	.927	.971	.871	.946
R6	85.8	218	102.0	.894	.959	.949	.887	.869	.922	.828	.918	.910	.833	.877	.824
R7	53.9	52.2	145.9	.709	.724	.833	.732	.710	.844	.650	.716	.798	.698	.691	.845
R8	40.4	86.6	121.3	.750	.958	.875	.768	.942	.880	.688	.933	.841	.710	.897	.812
R9	40.4	190.4	86.4	.741	.825	.860	.756	.872	.861	.674	.792	.826	.716	.794	.856
B1	136.	0	154.1	.877	–	.972	.898	–	.977	.822	–	.940	.872	–	.962
B2	138.	57.1	188.	.906	1.182	.815	.913	1.147	.826	.860	1.157	.823	.873	1.076	.792
B3	140.	165.1	161.6	.954	.833	.879	.961	.806	.858	.906	.815	.860	.916	.755	.771
B4	153.	268.	147.7	.991	.924	.852	.979	.915	.843	.885	.878	.806	.979	.901	.830
B5	156.	424.	0	.924	.879	–	.917	.856	–	.869	.860	–	.880	.809	–
B6	109.	0	194.2	.851	–	1.004	.833	–	.989	.765	–	.953	.819	–	.965
B7	96.2	67.8	179.1	.917	.880	.912	.930	.867	.911	.859	.860	.882	.896	.835	.887
B8	92.2	171.3	147.1	.996	.883	.923	1.022	.882	.930	.933	.859	.890	.983	.861	.906
B9	99.2	243.	155.6	.841	.940	.874	.837	.931	.867	.758	.896	.826	.819	.910	.848
B10	119.	455.	0	1.155	1.001	–	1.103	.951	–	1.066	.963	–	1.014	.845	–
B11	60.7	0	165.5	.817	–	.929	.823	–	.929	.743	–	.890	.795	–	.910
B12	57.1	64.4	168.0	.756	.639	.854	.771	.638	.860	.670	.616	.809	.750	.627	.849
B13	53.2	252.	128.8	.942	.876	.915	.930	.861	.900	.856	.840	.875	.867	.819	.857
B14	58.4	372.	0	.800	.886	–	.799	.879	–	.747	.861	–	.737	.840	–
Mean Value				.877	.899	.905	.878	.879	.899	.807	.873	.868	.842	.836	.867
Std. Deviation				.105	.108	.055	.097	.099	.051	.102	.105	.048	.094	.090	.057
Coeff. Variation				.011	.011	.003	.009	.009	.002	.010	.011	.002	.008	.008	.003

1 K. = 4.5 kN 1 K-ft = 1.37 kN-m.

concrete. Two factors can be suggested to explain why. First the "failure" strains represented the average of strains through a 30-inch length of the specimen before failure occurred but locally at the failure zone, strains were larger. Second, the spacing of longitudinal bars and transverse ties may have provided effective lateral confinement of concrete in corners or rounded ends of specimens. Among the 4 stress-strain functions for concrete, the parabola-rectangle and the modified Hognestad function (parabola-trapezoid) gave forces slightly closer to those measured than did the Chang or the Kent and Park functions. Any of the 4 functions could be used to generate a satisfactory thrust and moment capacity interaction surface. However, most design circumstances do not justify the implementation of a non-linear analysis of discretized cross-sections as a normal part of the design process.

The normal design process would employ handbook aids or computer programs for estimating uniaxial thrust and moment capacity of cross sections. Most design aids are derived with a rectangular stress block (Reference 4) to represent plain concrete at ultimate load. The same type interaction diagrams for uniaxial bending capacity about each principal axis of test specimens were derived, and test loads were compared with the capacities, as tabulated in Table C. When the failure thrust P_u is acting the flexural capacities M_{nx} and M_{ny} are bending capacities one would obtain from design aids if such aids were available with a capacity reduction factor $\phi = 1$ for the specific values γ, f'_c, and f_y for each specimen. Eccentricities e_{ux} and e_{uy} are quotients obtained by dividing ultimate midheight moments M_{ux} and M_{uy} by the failure thrust P_u.

Two forms of an analytic function for the strength interaction surface are examined with data in Table C. Planes of constant thrust would intercept the strength interaction surface along "contours" that relate moment capacities about each principal axis. If the contours were taken to be elliptical in shape the biaxial moment capacities M_{ux} and M_{uy} would be related to uniaxial capacities M_{nx} and M_{ny} as follows:

$$\left(\frac{M_{ux}}{M_{nx}}\right)^2 + \left(\frac{M_{uy}}{M_{ny}}\right)^2 = 1 \qquad (1a)$$

The distance from the center of the ellipse to a point on the ellipse is the square root of the left side of Eq. (1), and these distances represent resultant moment capacity. The square root of the left side of Eq. (1) can be taken as ratios between test load and load predicted by Eq. (1). The ratios are listed in the 4th column of Table C. All values exceed 1, and the average of 14 values for skew bending conditions was 1.15. The smallest values occur when the skew loading angle approached 45 degrees and axial loads were less than 0.5 P_o, but the hint of a deviation from the elliptical shape of the interaction function is not large enough to justify a complex evaluation of

TABLE C Analysis of Section Capacity

Specimen	Elliptical Moment Contours			Reciprocal Thrust Equation						
	M_{nx} in-k	M_{ny} in.k	$\sqrt{\left(\frac{M_{ux}}{M_{nx}}\right)^2+\left(\frac{M_{uy}}{M_{ny}}\right)^2}$	$\frac{P_u}{P_o}$	e_{ux} in.	e_{uy} in.	$\frac{P_x}{P_o}$	$\frac{P_y}{P_o}$	P_i k	$\frac{P_u}{P_i}$
R1	257.	140.	1.34	0.541	0.51	1.55	0.875	0.407	84.6	1.41
R2	255.	139.	1.21	0.548	1.03	1.28	0.759	0.509	96.0	1.25
R3	262.	143.	1.25	0.561	1.78	0.99	0.606	0.600	99.3	1.30
R4	284.	155.	1.05	0.389	0.46	1.85	0.883	0.376	80.2	1.09
R5	291.	158.	1.05	0.406	1.36	1.59	0.687	0.423	82.3	1.15
R6	271.	148.	1.06	0.405	2.54	1.19	0.485	0.542	72.9	1.18
R7	245.	136.	1.09	0.267	0.97	2.71	0.769	0.239	45.0	1.20
R8	225.	123.	1.06	0.203	2.14	3.00	0.550	0.213	36.1	1.12
R9	227.	124.	1.09	0.199	4.71	2.14	0.251	0.330	33.8	1.20
B1	330.	137.	1.13 *	0.581	0	1.13	0	0.542	126.8	1.07*
B2	327.	137.	1.38	0.595	0.41	1.36	0.919	0.474	105.6	1.31
B3	322.	133.	1.32	0.606	1.18	1.15	0.795	0.535	108.6	1.29
B4	385.	158.	1.17	0.560	1.75	0.97	0.687	0.586	126.3	1.21
B5	332.	135.	1.28*	0.629	2.72	0	0.539	0	133.6	1.17*
B6	428.	177.	1.10*	0.394	0	1.78	0	0.362	99.9	1.09*
B7	392.	163.	1.11	0.406	0.70	1.86	0.859	0.373	83.3	1.16
B8	370.	155.	1.06	0.399	1.86	1.60	0.678	0.417	80.4	1.15
B9	408.	170.	1.09	0.382	2.45	1.57	0.574	0.413	82.2	1.21
B10	424.	175.	1.07*	0.428	3.82	0	0.403	0	112.0	1.06*
B11	372.	158.	1.05*	0.246	0	2.73	0	0.231	57.1	1.06*
B12	366.	155.	1.10	0.232	1.13	2.94	0.801	0.209	48.9	1.17
B13	364.	153.	1.09	0.214	4.74	2.42	0.335	0.265	43.2	1.23
B14	354.	151.	1.05*	0.253	6.37	0	0.242	0	55.9	1.05*
Average (Skew bending)			1.15	1 in-k = 0.114 kN-m			1 k = 4.5 kN			1.21
Std. deviation			0.11	1 in = 25.4 mm						0.08

* Values for uniaxial bending are not included in statistical calculation.

new exponents less than 2. When the traditional rectangular stress block represents concrete in strength estimates, Eq. (1) underestimated actual skew bending capacity by an average amount of 15 per cent.

The second analytical function that was examined in Table C is the reciprocal thrust relationship.

$$\frac{1}{P_i} = \frac{1}{P_x} + \frac{1}{P_y} - \frac{1}{P_o} \tag{2}$$

in which P_i is the thrust capacity at an inclined eccentricity with respect to the principal axes, P_x is the thrust capacity if the eccentricity about the y-axis were zero, P_y is the thrust capacity if eccentricity about the x-axis were zero, and P_o is the squash load under no eccentricity. Values of P_x and P_y were obtained from the same interaction functions that were used for values of M_{nx} and M_{ny}. All of the estimated skew bending capacities P_i were lower than test loads P_u, and ratios of the values P_u/P_i show in the right hand column of Table C. The average ratio for the 14 skew bending cases was 1.21, indicating that biaxially eccentric thrust capacity was estimated by Eq. (2) to be 21 per cent less than that observed when the usual rectangular stress block is used to represent concrete capacity at failure under uniaxial loading conditions. The thrust relationship of Eq. (2) did produce results with a standard deviation smaller than that observed for the moment relationship of Eq. (1a)

EFFECTS OF SLENDERNESS

The effects of slenderness can be observed from values of the ratio between end moment and midheight moment. These ratios are observed moment magnification factors based on the condition of the specimens just before failure occurred. The moment magnification expression of the Building Code (10) can be rearranged to provide values of an apparent effective stiffness EI_{eff} as follows:

$$EI_{eff} = \frac{P_u \ell^2}{\pi^2 \left(\frac{M_\ell}{M_{end}} \right)} \tag{3}$$

Analytic expressions for the stiffness function EI appear in the ACI Building Code in the form of a fraction α of nominal gross stiffness of concrete $E_c I_G$ and in the form of steel stiffness $E_s I_s$ plus a different fraction β of the gross stiffness of concrete:

$$EI_1 = \alpha E_c I_G \tag{4a}$$

$$EI_1 = E_s I_s + \beta E_c I_G \tag{4b}$$

Values of α and β that correspond with test data can be determined with the substitution of Eq. (4a) and (4b) into Eq. (3) to obtain:

$$\alpha = \frac{P_u \ell^2}{\pi^2 \left(1 - \frac{M_{\ell}}{M_{end}}\right) E_c I_G} \tag{5a}$$

$$\beta = \frac{P_u \ell^2}{\pi^2 \left(1 - \frac{M_{\ell}}{M_{end}}\right)} - E_s I_s \frac{1}{E_c I_G} \tag{5b}$$

Table D contains maximum values of the ratio M_{ℓ}/M_{end} and calculated values of α and β for all specimens. The graphs of Fig. 5 display variations of α and β for the different amounts of axial load reflected by ratios P_u/P_o. "Observed" values of effective stiffness were found generally to be lower than those obtained from ACI Code Eq. 10-10, as shown in Fig. 4(a), and Fig. 4(b), indicating that the majority of "observed" values of effective stiffness were less than those obtained from Eq. 10-9. In order conservatively to include a larger proportion of the measured values for an effective stiffness EI, the following expressions are suggested:

$$EI_1 = \frac{2}{3} \frac{P_u}{P_o} E_c I_g \geq 0.2 E_c I_G \tag{6a}$$

$$EI_2 = E_s I_s + \left(\frac{1}{3} \frac{P_u}{P_o} - \frac{1}{7.5}\right) E_c I_G \geq E_s I_s \tag{6b}$$

Actually, the apparent non-conservative influence of stiffness estimates EI overall may not lead to unsafe predictions of slender column capacity. The "measured" values of M_{ℓ}/M_{end} do involve the most exaggerated condition of response possible as the ultimate load state approached. Softening of the mid-height region prior to failure was more advanced in test specimens than in the conditions generally assumed as an analytic part of column failure. The measured surface strains listed in Table A exceeded the 0.3 per cent strain limit associated with failure conditions defined by regulations of the Building Code (10). Acceptable estimates of EI must be coordinated with the definition of failure. If failure were defined as a maximum value of M_u for each P_u as curvature increases, then the low reinforcement ratio of laboratory specimens tends to emphasize the variation of stiffness EI as cracking occurs, and the apparent influence of thrust ratios P_u/P_o may be smaller in the presence of higher amounts of longitudinal reinforcement.

TABLE D

Effective Stiffness Coefficients

$EI_{meas.} = \alpha E_c I_g$ ACI Code Eq. (10-10)

$EI_{meas.} = E_s I_s + \beta E_c I_g$ ACI Code Eq. (10-9)

Specimen	Strong axis bending			Weak axis bending		
	$\frac{M_\ell}{M_{end}}$	α	β	$\frac{M_\ell}{M_{end}}$	α	β
R1	1.276	0.265	0.029	1.487	0.567	0.360
R2	1.153	0.436	0.199	1.722	0.447	0.240
R3	1.174	0.407	0.178	1.978	0.393	0.192
R4	1.185	0.265	0.032	1.639	0.344	0.140
R5	1.123	0.401	0.173	1.555	0.399	0.199
R6	1.143	0.337	0.096	1.643	0.349	0.138
R7	1.090	0.330	0.082	1.456	0.282	0.065
R8	1.109	0.210	-0.041	1.402	0.233	0.014
R9	1.084	0.263	0.015	1.309	0.280	0.063
B1	–	–	–	1.643	0.567	0.351
B2	1.313	0.211	-0.086	1.774	0.519	0.301
B3	1.161	0.369	0.071	1.881	0.491	0.273
B4	1.150	0.387	0.118	1.618	0.594	0.398
B5	1.128	0.479	0.195	–	–	–
B6	–	–	–	1.780	0.367	0.171
B7	1.147	0.262	-0.023	1.633	0.389	0.181
B8	1.165	0.238	-0.060	1.496	0.457	0.239
B9	1.146	0.264	-0.012	1.569	0.418	0.215
B10	1.132	0.333	0.067	–	–	–
B11	–	–	–	1.370	0.355	0.145
B12	1.088	0.248	-0.038	1.382	0.327	0.117
B13	1.086	0.234	-0.050	1.354	0.319	0.111
B14	1.101	0.233	-0.065	–	–	–

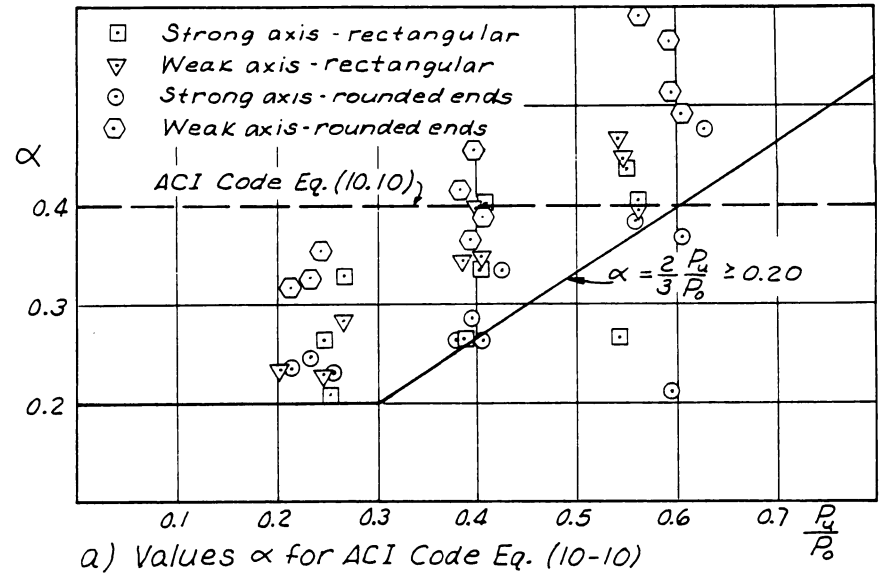

a) Values α for ACI Code Eq. (10-10)

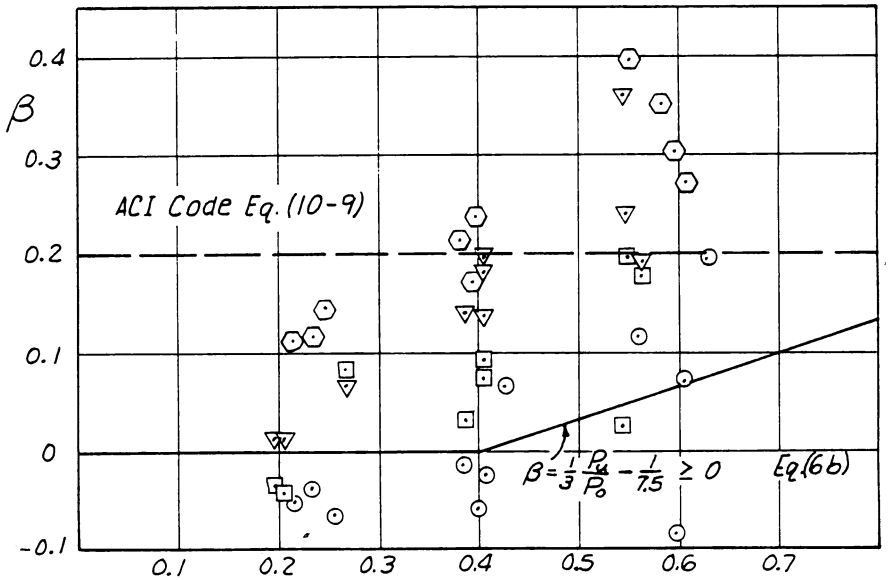

(b) Values β for ACI Code Eq. (10-9)

Fig. 5--Effective stiffness EI

Evidence from the tests does indicate that biaxially eccentric thrust slenderness effects can be analyzed separately for each principal axis. The capacity estimates must be developed from the combined thrust and magnified moments at the location involving the largest magnification of end moment, the midheight region for test specimens.

RECOMMENDATION FOR DESIGN

Analysis of data obtained in the 17 tests of columns that were subjected to biaxially eccentric thrust indicates that Eq. (1a) provided the most accurate description of cross section strength when concrete strength for major axis eccentricity was represented by a rectangular stress block and a limit strain of 0.003. When used with the same definition of cross section strength, Eq. (2) produced results consistently lower than those observed in test specimens. Tests indicated that the simple ellipse of Eq. (1a) gave good results. If the exponent were reduced from 2 to smaller values, the correlations with test results could be improved by less than 5 per cent. The complexity of modifying exponents different from those of the ellipse as in Eq. (1) is not justified by test results.

Slenderness effects could be evaluated separately for bending about each principal axis in order to obtain critical combinations of biaxial bending at midheight. The ACI Building Code recommendations for computing flexural stiffness EI produced values of appropriate order of magnitude, but values frequently were greater than those obtained from lateral deformations prior to failure of test specimens. For purposes of design, it appeared that the EI recommendations of the Building Code would lead to safe results if the cross section strength were analyzed on the basis of a limit strain of 0.003 and a rectangular representation of concrete stress failure.

A modification of Eq. (1a) can be used as a part of a simple and reliable design procedure. Cross sections can be proportioned for a resultant moment M_{ur} considered to act only about the major axis. For a rectangular, or even a circular end cross section of length a and width b, the ratio M_{nx}/M_{ny} can be taken roughly equal to a/b to yield

$$1 = \frac{1}{M_{nx}^2}\sqrt{M_{ux}^2 + \left(\frac{M_{nx}}{M_{ny}}\right)^2 M_{uy}^2} \qquad (1a)$$

$$M_{ur} = M_{nx}\sqrt{M_{ux}^2 + \frac{a^2}{b^2} M_{uy}^2} \qquad (7)$$

Reinforcement adequate to resist M_{ur} acting about the major axis should be spaced uniformly around the periphery of cross sections thus proportioned. After cross sections have been selected the specific values of M_{nx} and M_{ny} can be obtained with the aid of the

standard tables (12) or graphs (13) in order to demonstrate that Eq. (1) is satisfied by the selected section. An alternate and obviously more certain verification of an adequate selection could be based on Eq. (2). If values of P_o, P_x, and P_y for the chosen cross section produce a value P_i greater than that required, the cross section should be quite safe.

In order to demonstrate the reliability of Eq. (1) and Eq. (2) with ACI Building Code stiffness relationships (Eq. (4) with $\alpha = 0.40$ and $\beta = 0.20$), the 55 test specimens reported by Ramamurthy (20) were checked against analytic results. Test specimens with slenderness ratios ℓ_u/h from 6.25 to 12.5 were subjected to biaxially eccentric thrust applied at each end. The reinforcement ratios of all specimens were large enough that stiffness values EI from Eq. (4b) (ACI Code Eq. 10-9) were larger than those from Eq. (4a) (ACI Code Eq. 10-10). In order to compute analytical estimates of capacity, an iterative procedure was employed. An initial value of thrust was used to determine a moment magnification factor as well as a moment capacity for each axis of bending. If Eq. (1) was not satisfied, a different thrust was used until Eq. (1) was satisfied. Moment magnification factors were applied to end eccentricities before values P_x and P_y could be determined for use with Eq. (2). When the value of P_i from Eq. (2) was the same as that assumed for the determination of moment magnifiers, Eq. (2) was considered to be solved. Table E contains a listing of Ramamurthy's test specimens and a display of analytic results. Ratios between test loads P_{TEST} and computed capacities P_u are shown in the 10th and 15th columns of the table. The elliptic formula Eq. (1a) produced an average ratio P_{TEST}/P_u equal to 1.09, and (unsafe) ratios less than 1.00 were detected for only 7 of the 55 specimens. The reciprocal thrust formula Eq. (2) produced an average ratio P_{TEST}/P_u equal to 1.29, and none of the predictions were unsafe.

All results show that designers should be permitted to use Eq. (2) as a demonstration that a column loaded with biaxially eccentric thrust has been proportioned adequately. Whereas the use of a rectangular stress block for concrete strength and an analysis of cross section capacity has been shown by research reported here to be safe, the simpler use of Eq. (2) should be authorized explicitly by the ACI Building Code. The research reported here has illustrated that the equally simple ellipse Eq. (1a) produced more accurate correlations with observed and reported test results, but in 7 of the 72 specimens involving biaxially eccentric loads the predicted capacity exceeded the test load. If the exponent of terms in Eq. (1a) were changed from 2 to 1.5 in order always to produce analytic results greater than observed results, the average value of predicted results would be at least as (conservatively safe) far above test values as were those obtained from the reciprocal thrust Eq. (2).

TABLE E - Ramamurthy 8-Bar Specimens (Reference 19)

Test No.	Specimen	f'_c / $.85f_{cu}$ ksi	End Eccentricity e_x in	End Eccentricity e_y in	P_{test} K	Eqn. ① Analysis $\left(\frac{M_{ux}}{M_{nx}}\right)^2$	Eqn. ① Analysis $\left(\frac{M_{uy}}{M_{ny}}\right)^2$	Eqn. ① Analysis P_{u1} K	Eqn. ① Analysis $\frac{P_{test}}{P_{u1}}$	Eqn. ② Analysis P_x K	Eqn. ② Analysis P_y K	Eqn. ② Analysis P_{u2} K	Eqn. ② Analysis $\frac{P_{test}}{P_{u2}}$
A1	8in×8in	6.42	0.93	3.48	127.	0.067	0.933	110	1.16	256	114	98	1.30
2	f_y=42.3ksi	7.02	1.34	5.00	89.	0.067	0.933	76	1.17	233	79	68	1.31
3	ρ_g=0.025	6.60	1.34	5.00	85.	0.067	0.933	74	1.15	224	77	66	1.29
4	$k\ell$=80in	5.90	1.61	6.00	63.8	0.067	0.933	58	1.10	192	60	52	1.23
5		5.26	1.88	7.00	53.	0.067	0.933	47	1.13	166	49	42.5	1.25
6		4.96	2.06	7.98	38.6	0.063	0.937	40	0.97	152	41.5	36.2	1.07
7		5.49	2.00	10.00	33.	0.038	0.962	33	1.00	164	33.5	30.1	1.09
8		3.93	1.09	3.00	107.	0.117	0.883	98	1.09	177	105	87	1.23
9		5.70	2.18	6.00	63.	0.117	0.883	55.5	1.14	160	59.5	49	1.28
10		6.83	2.02	3.50	104.	0.250	0.750	100	1.04	185	130	93	1.12
11		7.08	2.89	5.00	59.5	0.250	0.750	67	0.89	151	79	59	1.01
12		6.12	4.04	7.00	38.2	0.250	0.750	44	0.87	95	51.3	36.4	1.05
13		2.57	4.00	6.00	37.	0.308	0.692	36	1.02	65.2	43.6	30.0	1.23
14		3.66	4.00	8.00	36.	0.200	0.800	33	1.09	71.5	31.9	24.1	1.49
15		2.92	3.54	3.54	60.	0.500	0.500	56	1.09	77.5	77.5	46.9	1.28
B1	8in×8in	4.00	0.83	3.09	141.4	0.067	0.933	124	1.14	231	126	109	1.30
2	f_y=46.8ksi	3.53	0.76	1.85	173.5	0.146	0.854	151	1.15	220	157	132	1.31
3	ρ_g=0.039	4.59	2.00	3.46	120.	0.250	0.750	111	1.08	174	126	92	1.30
4	$k\ell$=80in	4.38	2.50	4.33	89.	0.250	0.750	88	1.01	150	101	73	1.22
5		2.68	1.41	1.41	134.5	0.500	0.500	131	1.03	153	153	109	1.23
6		3.77	2.55	2.55	112.5	0.500	0.500	111	1.02	137	137	88	1.28
7		4.04	2.83	2.83	116	0.500	0.500	106	1.09	134	134	84	1.38
8		4.68	4.00	4.00	83.1	0.500	0.500	79	1.05	112	112	66	1.26
C1	6in×6in	4.27	0.39	1.45	104.5	0.067	0.933	92	1.13	149	94	83	1.26
2	f_y=40.0ksi	4.65	0.47	1.74	90.	0.067	0.933	87	1.03	150	89	77.5	1.16
3	ρ_g=0.044	3.97	0.75	1.30	103.5	0.250	0.750	89	1.16	120	96	76	1.36
4	$k\ell$=60in	3.30	0.90	1.56	85.	0.250	0.750	73	1.17	101	79	61	1.39
5		3.40	0.85	0.85	113.8	0.500	0.500	91	1.25	105	105	77	1.48
6		4.25	1.70	1.70	78.8	0.500	0.500	62	1.26	86	86	56	1.41

1 in = 25.4 mm 1 ksi = 6.98 MPa 1 in-k = 0.114 kN-m 1 k = 4.5 kN

TABLE E (continued)

Test No.	Specimen	f'_c $.85f_{cu}$ ksi	End Eccentricity e_x in	e_y in	P_{test} k	Eqn. ① Analysis $\left(\frac{M_{ux}}{M_{nx}}\right)^2$	$\left(\frac{M_{uy}}{M_{ny}}\right)^2$	P_{u1} k	$\frac{P_{test}}{P_{u1}}$	Eqn. ② Analysis P_x k	P_y k	P_{u2} k	$\frac{P_{test}}{P_{u2}}$
C1a		5.07	0.39	1.45	128	0.067	0.933	101	1.26	166	103	91	1.41
C2a		5.95	0.47	1.74	110	0.067	0.933	99	1.11	174	101	87	1.26
R138	6in×6in	3.19	3.00	3.00	31.1	0.500	0.500	27.0	1.15	38.4	38.4	22.5	1.38
238	f_y=40.0ksi	4.25	3.00	3.00	36.0	0.500	0.500	30.4	1.19	43.7	43.7	23.3	1.42
338	ρ_g=0.024	4.46	3.00	4.49	26.7	0.308	0.692	24.0	1.11	45.0	29.3	19.8	1.35
438	ℓ_k=60in	3.72	4.00	6.00	16.0	0.308	0.692	16.5	0.97	20.0	16.5	9.6	1.67
D1	6in×9in	4.34	1.50	1.00	176.5	0.352	0.633	158.	1.12	192.	167.	126.	1.40
2	f_y=46.8ksi	3.48	3.33	2.22	90.	0.397	0.603	89.5	1.01	117.	100.	67.	1.34
3	ρ_g=0.046	3.35	4.50	3.00	70.	0.415	0.572	65.	1.08	95.	82.	53.	1.32
4	ℓ_k=75in.	3.44	1.27	1.27	153.	0.209	0.795	133.	1.15	182.	135.	109.	1.40
5		4.23	3.18	3.18	85.	0.304	0.663	85.	1.00	131.	86.5	63.	1.35
6		3.27	1.80	3.12	90.	0.091	0.909	79.5	1.13	155.	79.	66.	1.36
E1	6in×12in	3.21	4.50	2.25	104.5	0.359	0.631	101.	1.03	137.	112.	77.	1.36
2	f_y=46.8ksi	2.93	6.00	3.00	70.	0.395	0.610	71.	0.99	109.	89.	59.	1.19
3	ρ_g=0.034	3.80	3.39	3.39	98.	0.141	0.867	82.	1.20	176.	92.	73.	1.34
4	ℓ_k=75in	3.40	1.50	2.06	122.	0.045	0.963	109.	1.20	231.	105.	93.	1.31
F1	6in×9in	4.01	2.17	0.58	135.	0.781	0.228	128.	1.05	130.	162.	102.	1.32
2	f_y=42.3ksi	4.92	1.87	1.25	120.	0.360	0.611	125.	0.96	158.	134.	97.	1.24
3	ρ_g=0.030	2.46	1.87	1.25	86.5	0.381	0.623	85.	1.02	104.	92.	67.	1.29
4	ℓ_k=75in.	3.47	3.00	2.00	60.	0.410	0.589	71.	0.85	100.	86.	58.	1.03
5		3.65	1.59	1.59	105.	0.212	0.779	99.	1.06	142.	101.	79.	1.33
G1	6in×12in	4.52	2.90	0.78	186.	0.603	0.395	166.	1.12	181.	192.	129.	1.44
2	f_y=42.3ksi	3.47	4.83	1.29	94.	0.663	0.342	103.	0.91	112.	132.	78.	1.21
3	ρ_g=0.022	2.81	2.68	1.34	114.	0.338	0.650	111.	1.03	144.	118.	88.	1.30
4	ℓ_k=75in	5.11	5.37	2.68	75.	0.423	0.577	71.5	1.05	121.	94.	62.	1.21
5		4.26	1.70	1.70	131.5	0.129	0.856	130.	1.01	219.	128.	108.	1.22
55 Specimens						Average			1.08				1.29
						Std. Dev.			0.09				0.12

CONCLUSIONS

Test results have been displayed for 23 reinforced concrete columns of rectangular or partially circular cross sections subjected to eccentric compression loading. Comparisons between measured displacements, strains and strength and analytically derived displacements, strain and strength indicated that:

1. The difference between the skew angle of the neutral axis increased as the skew angle of loading departed from the minor axis. Small eccentricities from the major axis could produce comparably large differences between skew loading angle and neutral axis angle, but the implied tendency to twist longitudinally about the axis of the column was almost impossible to detect.

2. Integration of stresses compatible with measured strains showed clearly that the rectangular stress block representation of concrete at ultimate undervalued cross section strength when the compression zone was not rectangular at failure. The use of a parabola-trapezoidal stress-strain function produced results more closely in agreement with observed results than did the use of other analytic stress-strain functions for concrete.

3. The contours to an interaction surface at constant thrust appeared to conform to an elliptic shape.

4. The reciprocal thrust Eq. (2) produced strength estimates 21 per cent greater than those observed, and none of the elements was lower than the observed thrust.

5. Effective values of flexural stiffness EI were evaluated from measurements of transverse displacement just before columns failed. The apparent values of EI appeared to increase as ratios of average axial strength P_u/P_o increased. Equations acceptable by ACI 318-77 produced values generally greater than those derived from test data.

6. Strength estimates were derived from traditional (rectangular stress block) thrust and uniaxial moment capacity functions for stiffness EI, and biaxial bending interaction functions Eq. (1) and Eq. (2). The elliptical moment ratio function of Eq. (1) produced strength estimates with average values 15 per cent lower than those observed, and the reciprocal thrust function of Eq. (2) produced strength estimates with average values 21 per cent lower than the observed strengths.

7. A comparison between the observed strength and the use of Eq. (2) and Eq. (1) for estimates of capacity of 55 specimens reported by Ramamurthy produced results similar to those for the 17 new tests reported in this paper.

8. If slenderness effects are evaluated separately for each principal plane of bending in accordance with recommendations

of ACI 318-77, and if traditional handbook (12, 13) thrust-moment interaction functions are used for cross section strength, the reciprocal thrust Eq. (2) produced safe estimates of capacity for all 73 test specimens studied. The use of Eq. (2) should be authorized explicitly by the ACI Building Code as an adequate analysis of skew bending strength of columns.

REFERENCES

1. ACI Committee 105, F. E. Richart, Chairman, "Reinforced Concrete Column Investigation, Tentative Final Report", Journal of American Concrete Institute, Feb., 1933.

2. Large, George E., Basic Reinforced Concrete Design, 2nd Ed., Ronald Press, 1957, p. 80.

3. Reinforced Concrete Design Handbook, (ACI 317-55) American Concrete Institute, Detroit, pp. 66-71.

4. Building Code Requirements for Reinforced Concrete (ACI 318-63), American Concrete Institute, Detroit, 1977, Clause 10.2.7.

5. Berwanger, Carl, "Effect of Axial Load on the Moment-Curvature Relationship of Reinforced Concrete Members", Reinforced Concrete Columns (SP5D) American Concrete Institute, Detroit, 1975, p. 271.

6. Warner, R. F., "Biaxial Moment Thrust Curvature Relations", Journal of Structural Division, American Society of Civil Engineers, ST 5, May, 1965, pp. 923-940.

7. Farah, A., and Huggins, M. M., "Analysis of Reinforced Concrete Columns Subjected to Longitudinal Load and Biaxial Bending", Journal of American Concrete Institute, Vol. 66, No. 7, July, 1969, pp. 569-575.

8. Drysdale, R. G., and Huggins, M. W., "Sustained Biaxial Load on Slender Concrete Columns", Journal of the Structural Division, American Society of Civil Engineers, ST5, May, 1971, pp. 1423-1443.

9. Wu, H. and Huggins, M. W., "Size and Sustained Load Effects in Concrete Columns", Journal of the Structural Division, American Society of Civil Engineers, ST3, March, 1977, pp. 493-506.

10. Building Code Requirements for Reinforced Concrete (ACI 318-77) American Concrete Institute, Detroit, 1977.

11. Standard Specifications for Highway Bridges, The American Association of State Highway Officials, Eleventh Edition, 1973, p. 80.

12. Design Handbook - Columns, Vol. 2 (SP17A), American Concrete Institute, Detroit, 1978.

13. CRSI Handbook, Concrete Reinforcing Steel Institute, Chicago, 1979.

14. Advanced Engineering Bulletin No. 20, "Biaxial and Uniaxial Capacity of Rectangular Columns", Portland Cement Association, Skokie, Illinois, 1967.

15. Pannell, F. N., "Failure Surfaces for Members in Compresion and Biaxial Bending", Journal of American Concrete Institute, January 1963, pp. 129-140.

16. Mavichak, V., and Furlong, R. W., "Strength and Stiffness of Reinforced Concrete Columns Under Biaxial Bending", Research Report 7-2F, Project 3-5-73-7, Center for Highway Research, The University of Texas at Austin, Nov. 1976.

17. Hognestad, E., "A Study of Combined Bending and Axial Load in Reinforced Concrete Members", University of Illinois Engr. Exp. Sta., #399, Urbana, 1951.

18. Kent, D. C. and Park, R., "Flexural Members With Confined Concrete", Journal of the Structural Division, American Society of Civil Engineers, ST7, July 1971, pp. 1969-1990.

19. Chang, Donald C., unpublished doctoral dissertation, The University of Texas at Austin, 1977.

20. Ramamurthy, L. N., "Investigation of the Ultimate Strength of Square and Rectangular Columns Under Biaxially Eccentric Loads", Symposium on Reinforced Concrete Columns, (ACI SP-13) American Concrete Institute, Detroit, 1966, pp. 263-298.

ACKNOWLEDGEMENT

The research described in this paper was carried out under a project "Design Parameters for Columns in Bridge Bents" supported by Texas State Department of Highways and Public Transportation in cooperation with the United States Department of Transportation Federal Highway Administration. The contents of the paper reflect the views of the author, who is responsible for the facts and accuracy of data presented. The contents do not necessarily reflect the official views or policies of the Federal Highway Administration.